

Magnetic correlations in two-dimensional spin-glasses

I. Morgenstern and K. Binder

Institut für Festkörperforschung der Kernforschungsanlage Jülich,

Postfach 1913, D-5170 Jülich, West Germany

(Received 6 February 1980)

By a recursive method numerically exact free energies are calculated for square $L \times L$ Ising lattices, with $6 \leq L \leq 18$, for several kinds of frozen-in bond disorder: (i) bonds $\pm J$ with various concentrations of negative bonds; (ii) bonds distributed according to a Gaussian distribution. Ground states of these systems are identified, the response to "ordering fields" is studied, and the correlation function $\langle S_0 S_R \rangle_T^2$ is calculated as a function of temperature for various distances R in the lattice. This correlation is found to decay strongly (presumably exponentially) with increasing R even at temperatures distinctly below the apparent freezing temperature T_f of previous Monte Carlo simulations; this "freezing transition" is hence unambiguously identified as a nonequilibrium effect. However, the correlation length is found to become long ranged at low temperatures, and it is suggested that a phase transition still occurs at $T=0$; while in the Gaussian model the spin-glass order parameter $q(T=0)=1$, it is found that $q \equiv 0$ in the $\pm J$ model where rather a power-law decay of correlations $\langle S_0 S_R \rangle_{T=0}^2$ occurs. Performing Monte Carlo simulations for precisely the same systems, the cooling times necessary to reach the true ground states of the system are identified, as well as the simulation times necessary to reach thermal equilibrium for the correlation functions. These times are found to increase so strongly with L that for systems of macroscopic size the correct thermal equilibrium is probably irrelevant for experimental purposes. Rather a statistical mechanics based on the many long-lived metastable states would be required.

I. INTRODUCTION

The appropriate theoretical description of spin-glasses is a problem of strong recent efforts and much controversy.¹⁻⁷ In their pioneering paper² Edwards and Anderson suggested that the frozen-in state of spin-glasses is characterized by a nonzero local order parameter $q = (\langle S_i \rangle_T^2)_{av}$, where $(\dots)_{av}$ means averaging over the quenched disorder. "Freezing" of the spins at the freezing temperature T_f would then be a phase transition like other phase transitions which occur in thermal equilibrium. It is this behavior which is believed to occur at least in the mean-field limit, although a mean-field theory which becomes rigorous for long-range random interactions has not yet been established.²⁻⁷ However, it is already clear that the mean-field predictions are not in agreement with experiment,⁸ and it is necessary to go beyond the mean-field limit. At present there is no consensus about what then happens:

(i) Monte Carlo simulations of Ising models where nearest neighbors have either a random Gaussian exchange⁹⁻¹¹ or exchange $\pm J$ (random-sign model)^{12,13} first were interpreted in accord with the Edwards-Anderson hypothesis. Anomalous slow relaxation phenomena, which are seen in the simulations,^{9-11,14} have then been interpreted as evidence against an

Edwards-Anderson transition.¹⁴ However, many arguments have been given¹⁵⁻¹⁷ that the interpretation of Ref. 14 is not conclusive—perhaps the most convincing argument being the similarity of the results obtained to those at $d=5$ spatial dimensions, where Edwards-Anderson transition is generally accepted. From various treatments^{16,18-21} it seems plausible that the simulations so far studied only the initial stages of relaxation towards equilibrium in these models, and hence have little bearing on the question of what happens in equilibrium. It is an open question to identify the times necessary to simulate equilibrium properties of spin-glasses.

(ii) The renormalization-group approach has also yielded quite ambiguous predictions for the lower critical dimensionality d_c , below which $T_f \equiv 0$. Real-space methods for Ising spin-glasses yielded^{22,23} $2 \leq d_c \leq 3$. The reliability of this approach is hard to ascertain, however. The more reliable ϵ expansion in terms of $\epsilon = d - d^*$ where d^* is the upper critical dimensionality ($d^* = 6$ here²⁴) relies on the replica method and an expansion in powers of q , which seems to be of doubtful validity below T_f as instabilities occur.^{25,26} A certain version of replica symmetry breaking removing some of these instabilities yields $d_c = 4$ (Ref. 27) but this scheme needs further justification.⁷ The result $d_c = 4$ seems to be corroborated

by high-temperature series expansions for both the $\pm J$ model²⁸ and the Gaussian model,²⁹ but these (relatively short) series are quite irregular and hence, hard to analyze. In addition, it is conceivable that the "susceptibility" $\chi_{EA} \equiv k_B T \sum_R (\langle S_0 S_R \rangle)^2$ remains finite at the spin-glass transition.¹⁵

(iii) A third approach concentrates on ground-state properties, starting from the fact that a considerable fraction of the bonds remains "frustrated."³⁰ Analysis of ground-state properties is useful to estimate the concentration of negative bonds for which one just can no longer have a ferromagnetic ground state.^{31-33,12} In addition, one finds that even for $d=2$ there are large "packets of solidary spins" in the spin-glass ground states, i.e., groups of spins that always keep the same relative orientation in the ground states.^{32,33} Since these packets overlap, the significance of this observation for the question if a transition occurs is not clear.³³ Also the suggestion that in spin-glasses for $d=2, 3$ the boundary energy at $T=0$ vanishes³⁴ does not give a conclusive answer to this question.³⁵ Finally we note that approaches where frustration is treated as a field in a continuum description^{36,37} have not settled this problem either: On the one hand, a fixed point corresponding to a transition to order like in a Mattis spin-glass³⁸ is shown to be unstable against frustration below $d=4$ (Ref. 37); on the other hand, for Heisenberg spin-glasses it was suggested that $d_c=3$ (Ref. 36), and one expects that in the Ising case d_c is the same³⁹ or lower.²² Note, however, that this gauge-field approach also needs further clarification.⁴⁰ Finally we note that at $T=0$ and $d=2$ a paramagnet-spin-glass transition was also identified from systematic series expansions for diluted spin-glasses.⁴¹

In the present paper, we wish to contribute to clarify some of these questions by studying the statistical mechanics of two-dimensional Ising spin-glasses more carefully. In Sec. II we describe methods to calculate the partition function of $L \times L$ lattices (with L up to 18) exactly, as well as certain response and correlation functions. In Sec. III the results for the $\pm J$ model are compared to Monte Carlo calculations for precisely the same systems, in order to unambiguously distinguish nonequilibrium phenomena from

equilibrium properties in the simulations.⁴² The time scales necessary to get meaningful equilibrium results are identified. In Sec. IV the same is done for the Gaussian model. Extrapolating our results for various L to $L \rightarrow \infty$ we conclude that neither of these models exhibits order at nonzero temperatures, but both of them have a transition at $T=0$. In Sec. V the transition ferromagnet-paramagnet is studied for the $\pm J$ model as function of temperature and concentration of the wrong bonds. Section VI contains our conclusions.

II. RECURSIVE METHODS TO CALCULATE PARTITION FUNCTIONS, SELECTED GROUND STATES, AND RESPONSE AND CORRELATION FUNCTIONS AT FINITE LATTICES

We consider the Ising Hamiltonian with arbitrary inhomogeneous nearest-neighbor interaction $\{J_{ij}\}$ and field $\{H_i\}$ for a $L \times K$ square lattice

$$\mathcal{H} = - \sum_{\langle i,j \rangle} J_{ij} S_i S_j - \sum_i H_i S_i \quad (1)$$

where the sums $\langle i,j \rangle$ run over nearest-neighbor pairs in the lattice. For computational reasons, which will become clear later, we apply periodic boundary conditions in the horizontal lattice direction (where the lattice linear dimension is L), but free boundary conditions in the vertical one (where the lattice linear dimension is K). We attempt to calculate the free energy numerically exact for one set of interaction parameters and fields $\{J_{ij}\}$, $\{H_i\}$, normalized per site; i.e.,

$$F_{\{J_{ij}\}, \{H_i\}} = - \frac{k_B T}{LK} \ln Z_{\{J_{ij}\}, \{H_i\}} \quad (2)$$

The problem of averaging Eq. (2) over the disorder in the system according to suitable distributions for $P(J_{ij})$ and/or $P(H_i)$ will be treated later. We first note that the partition function appearing in Eq. (2) can be written as follows, denoting by S_{kl} the spin in the k th line and l th column, and $\tilde{J} \equiv J/k_B T$, $\tilde{H} \equiv H/k_B T$, $J_{kl,mn}$ connecting spins S_{kl}, S_{mn} :

$$\begin{aligned} Z_{\{J_{ij}\}, \{H_i\}} = & \sum_{\{S_{11}\}} \sum_{\{S_{12}\}} \cdots \sum_{\{S_{1L}\}} \sum_{\{S_{21}\}} \cdots \sum_{\{S_{2L}\}} \cdots \sum_{\{S_{K1}\}} \cdots \sum_{\{S_{KL}\}} \\ & \times \left(\prod_{l=1}^L \exp(\tilde{J}_{1l, 1l+1} S_{1l} S_{1l+1}) \exp(\tilde{H}_{1l} S_{1l}) \exp(\tilde{J}_{1l, 2l} S_{1l} S_{2l}) \right) \\ & \times \left(\prod_{l=1}^L \exp(\tilde{J}_{2l, 2l+1} S_{2l} S_{2l+1}) \exp(\tilde{H}_{2l} S_{2l}) \exp(\tilde{J}_{2l, 3l} S_{2l} S_{3l}) \right) \times \cdots \\ & \times \left(\prod_{l=1}^L \exp(\tilde{J}_{Kl, Kl+1} S_{Kl} S_{Kl+1}) \exp(\tilde{H}_{Kl} S_{Kl}) \right) \end{aligned} \quad (3)$$

We compute $Z_{\{J_{ij}\}, \{H_i\}}$ recursively similar to a method applied earlier for homogeneous systems.⁴³ The first step is to compute the "horizontal factor"

$$\prod_{l=1}^L \exp(\tilde{J}_{1l, 1l+1} S_{1l} S_{1l+1}) \exp(\tilde{H}_{1l} S_{1l})$$

for all 2^L states of the $\{S_{1l}\}$. It is the storage requirement for this factor which prevented us from studying L larger than $L = 18$ (while there is much less difficulty to go to larger K). Then we calculate the first "vertical factor" $\exp(\tilde{J}_{11, 21} S_{11} S_{21})$ for the two possible choices of $S_{21} = \pm 1$. Since for our choice of boundary conditions we have then taken into account all interactions of S_{11} , we can already now perform the trace over S_{11} . For the further calculation we hence keep terms for all the states of $\{S_{1l, l > 2}\}$ and S_{21} . Then the second vertical factor $\exp(\tilde{J}_{12, 22} S_{12} S_{22})$ is calculated for the two states of S_{22} , and the trace over S_{12} is performed, etc. When S_{2L} is reached the trace over all $\{S_{1l}\}$ is completed and we now compute

the horizontal factor

$$\prod_{l=1}^L \exp(\tilde{J}_{2l, 2l+1} S_{2l} S_{2l+1}) \exp(\tilde{H}_{2l} S_{2l})$$

for all 2^L states of the $\{S_{2l}\}$. Adding the vertical factor $\exp(J_{21, 31} S_{21} S_{31})$ for the two states of S_{31} we may take the trace over S_{21} , and thus step by step take the trace over the spins in the second row, and after that of the third one, etc. Thus we obtain $Z_{\{J_{ij}\}, \{H_i\}}$ numerically for arbitrary values of the interaction parameters (and temperature T). By computing $\ln Z_{\{J_{ij}\}, \{H_i\}}$ for a set of neighboring temperatures we get internal energy per spin U and specific heat per spin C by numerical differentiation with very good accuracy. Similarly we can obtain arbitrary susceptibilities by recording the free energy for a set of neighboring values of the appropriate field and by taking the suitable derivative numerically.

It is also convenient to calculate correlation functions between the last spin (at site K, L) over which the trace is taken, and any other spin (at site i, j). We start from the identity

$$Z = \text{Tr}_{\{S_{11}, \dots, S_{KL}\}} \exp(-\mathcal{H}/k_B T) = \text{Tr}_{\{S_{11}, \dots, S_{KL-1}\}} \exp(-\mathcal{H}'/k_B T) (2 \cosh \tilde{H}_{KL}^{\text{eff}}) \text{Tr}_{S_{KL} = \pm 1} (1 + S_{KL} \tanh \tilde{H}_{KL}^{\text{eff}}) \quad (4)$$

where (assume $\tilde{H}_{KL} = 0$)

$$\tilde{H}_{KL}^{\text{eff}} \equiv \tilde{J}_{K-1, KL} S_{KL-1} + \tilde{J}_{KL, K+1} S_{K+1} + \tilde{J}_{K-1L, KL} S_{K-1L} \quad (5)$$

We now define a restricted partition function Z' , where the spin S_{KL} kept fixed at $S_{KL} = 1$, and hence note

$$Z' = Z (1 + \langle \tanh \tilde{H}_{KL}^{\text{eff}} \rangle) = Z (1 + \langle S_{KL} \rangle) \quad (6)$$

We now consider the derivatives with respect to a local field H_{ij} ,

$$\frac{\partial \ln Z'}{\partial \tilde{H}_{ij}} = \langle S_{ij} \rangle + \frac{\langle S_{ij} S_{KL} \rangle - \langle S_{ij} \rangle \langle S_{KL} \rangle}{1 + \langle S_{KL} \rangle} \quad (7)$$

$$\left. \frac{\partial^2 \ln Z'}{\partial \tilde{H}_{ij}^2} \right|_{\tilde{H}_{ij}=0} = 1 - \langle S_{ij} S_{KL} \rangle^2 \quad (8)$$

Hence the desired correlation function $\langle S_{ij} S_{KL} \rangle^2$, which when summed over all separations yields the susceptibility $k_B T \chi_{EA}$ mentioned in the introduction, is simply obtained by our method by computing restricted partition functions for a set of small \tilde{H}_{ij} close to $\tilde{H}_{ij} = 0$ to take the derivative defined in Eq. (8).

Somewhat more involved is the identification of ground states. We start by storing the n states of the first line having the lowest energies (typically $n \approx 10^2$). We combine these states with all 2^L states of the second line, and keep out of these $n 2^L$ states again n states, which now have the lowest energy.

This procedure is repeated line after line, until one completes all K lines, and one ends up with a set of n low-lying states for which the configurations of all K times L spins are known. We compare the total energy $U(m)$ for each of these remaining n states $\{m\}$ with the total ground-state energy $KL U(T=0) = KLF(T=0)$, which we obtain from Eqs. (2) and (3): If $U(m)$ equals this ground-state energy, then m is a ground state, while otherwise m is (at best) a low-lying metastable state. If it happens that no ground state is found for the chosen n (or too few of them), the procedure has to be repeated with larger n .

So far all results refer to one fixed set of interaction parameters $\{J_{ij}\}$ (and fields $\{H_i\}$). We wish to obtain average quantities

$$\langle \langle \dots \rangle \rangle_{\text{av}} = \prod_{(i,j)} \int dJ_{ij} P(J_{ij}) \langle \dots \rangle_{\{J_{ij}\}} \quad (9)$$

where $P(J_{ij})$ is the probability distribution which describes the bond disorder in the spin-glass.⁴⁴ In the $\pm J$ model, $P(J_{ij})$ is given by

$$P(J_{ij}) = (1-x) \delta(J_{ij} - J) + x \delta(J_{ij} + J) \quad (10)$$

i.e., x describes the concentration of negative bonds. In the Gaussian model, $P(J_{ij})$ is given by

$$P(J_{ij}) = (1/\sqrt{\pi}) \exp[-(J_{ij} - \bar{J})^2 / 2(\Delta J)^2] \quad (11)$$

\bar{J} being the mean and ΔJ the width of the distribution.

Unfortunately, it is impossible to perform also this averaging in Eq. (9) exactly in the cases we are interested in. Hence this averaging is done approximately, by generating a number M of characteristic realizations $\{J_{ij}\}$, where random numbers are used to generate $\{J_{ij}\}$ from the appropriate distribution [Eq. (10) or Eq. (11), respectively]. Hence Eq. (9) is replaced by

$$\langle \langle \dots \rangle \rangle_{\text{av}} = \frac{1}{M} \sum_{m=1}^M \langle \dots \rangle_{\{J_{ij}\}_m} \quad (12)$$

Since the various $\{J_{ij}\}_m$ are statistically independent of each other, also the averages $\langle \dots \rangle_{\{J_{ij}\}_m}$ are statistically independent quantities. Hence the error involved in replacing Eq. (9) by Eq. (12) is found from standard statistical analysis (these are the error bars quoted in the following sections).

It should also be noted that not all kinds of disorder lead to errors of this kind. Applying our method to the Mattis spin-glass, which is related to an Ising ferromagnet via gauge transformations,^{30,38} it is clear that all gauge-invariant quantities are obtained without any error from a single realization $\{J_{ij}\}$ already.

For the nontrivial distributions [Eqs. (10) and (11)] we again are interested in gauge-invariant correlations and susceptibilities only. For these quantities it is only the gauge-invariant part of the disorder which matters. On a square lattice this is not the concentration of negative bonds x , but rather the concentration of frustrated plaquettes x_F ,³⁰ which is related to x via (for an *infinite* system)

$$x_F = 4x(1-x)[x^2 + (1-x)^2] \quad (13)$$

Hence we have chosen our sets $\{J_{ij}\}_m$ for the

averaging in Eq. (12) such that they precisely satisfy Eq. (13) also in our *finite* systems [where Eq. (13) would hold on the average but not necessarily for each individual realization: in fact, since the Mattis disorder is a subclass of the disorder described by Eq. (10), for small x some realizations in a finite lattice would have no frustration at all, and hence yield very atypical results]. Hence, precisely speaking, we are not using Eq. (10) but rather a modified distribution $P'(J_{ij})$ defined by

$$P'(J_{ij}) = P(J_{ij}) \delta(x_F - 4x(1-x)[x^2 + (1-x)^2]) \quad (14)$$

$P'(J_{ij})$ reduces to $P(J_{ij})$ in the thermodynamic limit, and is a valid model distribution for disorder in a spin-glass as well as Eq. (10), of course. It turns out that use of Eq. (14) reduces the errors involved in Eq. (12) significantly, and between 15 and 100 realizations were sufficient to reach the accuracy shown here [direct use of Eq. (10) would have required about 10 times more computational effort to reach the same accuracy]. In the symmetric Gaussian model we also used a restricted distribution completely analogous to Eq. (14).

III. NUMERICAL RESULTS FOR THE SYMMETRIC $\pm J$ MODEL AND A COMPARISON WITH MONTE CARLO SIMULATIONS

For the symmetric $\pm J$ model we have $x = x_F = \frac{1}{2}$. Figure 1(a) shows internal energy U normalized *per bond* ($E = 2U$, and hence for periodic boundary conditions and/or infinite systems E is the internal energy normalized *per site*). Monte Carlo data were gen-

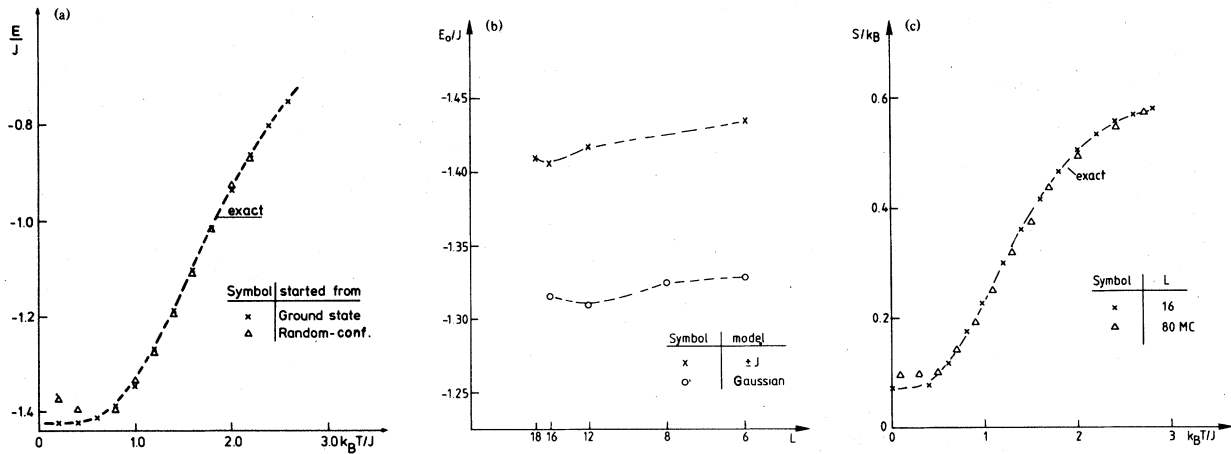


FIG. 1. (a) Internal energy of the symmetric $\pm J$ model plotted vs temperature for a 16×16 lattice. Dashed curve is the exact calculation, while the points denote Monte Carlo results. (b) Ground-state energy of the symmetric $\pm J$ and Gaussian $L \times L$ models plotted vs inverse linear dimension L . (c) Entropy plotted vs temperature. Triangles denote Monte Carlo results of Kirkpatrick (Ref. 12).

erated for precisely the same lattice (i.e., same size and same choice of the $\{J_{ij}\}$) and are included for comparison. Starting the Monte Carlo run from one of the ground states found from the exact calculation, it turns out that the energy always comes to equilibrium nicely, using an observation time of 20 000 Monte Carlo steps (MCS)/spin. The same is true for temperatures $k_B T/J \geq 0.8$ starting the simulation from a random initial spin configuration, while then for $k_B T/J \leq 0.4$ the deviation of the internal energy from its equilibrium value is quite pronounced.

There has been considerable discussion in the literature^{11, 12, 15, 16, 18, 20, 33, 34} concerning ground-state properties obtained from Monte Carlo simulations. Hence we investigated the circumstances under which one can reach true ground states from Monte Carlo simulations which are started with random initial states. We found the following procedure relatively efficient: the system is immediately quenched to a temperature somewhat above the apparent freezing temperature (which is about $k_B T/J \approx 1.4$ in this case¹²), e.g., to $k_B T/J = 1.8$, and from there the temperature is reduced linearly with time until zero temperature is reached after some chosen cooling time t_c . Then the system is allowed to evolve at $T = 0$ about 100 MCS/spin, and one asks whether the ground state has been reached.

It turns out that the t_c necessary to reach the ground state has a distinct dependence on the size of the system. Using $t_c = 10^5$ MCS/spin for a 6×6 lattice it turns out that the system not only reaches one of its ground states during the run but there are so many of them that one reaches for every one of them also the "opposite" one (which is constructed by changing signs of all the spins in the ground-state configuration). For 8×8 and 10×10 one no longer reaches both a ground state and its opposite one, but still $t_c > 10^5$ MCS/spin is sufficient to reach many ground states. Much shorter t_c (of order 10^3 to 10^4 MCS/spin) are sufficient to reach just one of them. For $N = 12 \times 12$ and 14×14 runs with $t_c = 10^4$ MCS/spin typically are no longer successful, one ends up with metastable states whose total energy is only slightly higher (e.g., by $2J$) than the true ground-state energy, but which differ from ground states by fairly large rearrangements of spin clusters. This observation is consistent with suggestions of Dasgupta *et al.*¹⁹ and Rammal *et al.*²⁰ With $t_c = 2 \times 10^4 - 3 \times 10^4$ MCS/spin one reaches the ground state in most cases, however, and the same is true for $N = 16 \times 16$. For $N = 18 \times 18$ $t_c = 2 \times 10^4$ was never found to be sufficient, and times $t_c = 3 \times 10^4 - 6 \times 10^4$ MCS/spin were needed. For $N = 24 \times 24$ a time $t_c = 8 \times 10^4$ MCS/spin are needed; and for $N = 32 \times 32$ even times $t_c = 1 \times 10^5 - 2 \times 10^5$ MCS/spin. Since we find the ground-state energy per bond to be weakly dependent on N , we estimate by

extrapolation [Fig. 1(b)]

$$E(T=0)/J = -1.4 \pm 0.01 \quad (15)$$

This estimate is slightly lower than previous Monte Carlo estimates^{12, 45}: on the basis of our observations we expect that in this work^{12, 45} no true ground states were reached but rather low-lying metastable states. The result of Ref. 31, where exact ground states are also generated is $E(T=0) \approx -1.4$, and hence in good agreement with our result. Figure 1(c) then shows the temperature variation of the entropy per spin. While at high temperatures our results agree well with the Monte Carlo estimates of Kirkpatrick,¹² our ground-state entropy is distinctly lower ($S/k_B \approx 0.075$) than his estimate [$S/k_B \approx 0.1$ (Ref. 12)]. The behavior of the energy as a function of size [Fig. 1(b)] suggests that the free boundaries allow the system to better "accomodate" to the disorder; i.e., "frustration" is less effective and hence we expect that our method slightly underestimates $S(T=0)$, as the ground-state degeneracy may be slightly reduced. However, Vannimenus and Toulouse³¹ obtain $S(T=0)/k_B = 0.07$ by a different method using lattices from 20×20 to 30×30 , which fact suggests that the Monte Carlo estimate is presumably somewhat too large.

The times necessary to lose the influence of the initial state at low temperatures ($k_B T/J \ll 1$) are of the same order as t_c . In order to obtain reasonable estimates for thermal averages, susceptibilities, etc., much larger observation times are needed, however. This is demonstrated in Fig. 2, where the Monte Carlo estimates of susceptibility $k_B T \chi(t)$ and an order parameter component $\psi_l^2(\{S_i^{(l)}\})$ being the spin configuration of the l th ground state) which is defined as¹¹

$$\psi_l^2(t) = \left[\frac{1}{N} \sum_i S_i^l S_i(t) \right]^2 \quad (16)$$

are plotted versus observation time t at a temperature below the apparent freezing temperature. It is seen that both $\chi(t)$ and $\psi_l^2(t)$ stay small up to about $t \approx 10^4$ MCS/spin while then a "transition" to another state occurs, where both $\chi(t)$ and $\psi_l^2(t)$ have nearly constant values for a time of order 10^4 MCS/spin, before again a transition occurs. We interpret observations of this kind as follows: Some of the ground states correspond to "valleys" in phase space, which are separated from each other by fairly high-lying saddle points. The transition seen in Fig. 2 corresponds to a trajectory of the system in its phase space passing over such a saddle point. If the system would stay in one valley in the thermodynamic limit an infinite time, the symmetry would be broken and the order parameter ψ (Ref. 11) would hence be nonzero. Comparison of the Monte Carlo data in finite systems with the corresponding exact results

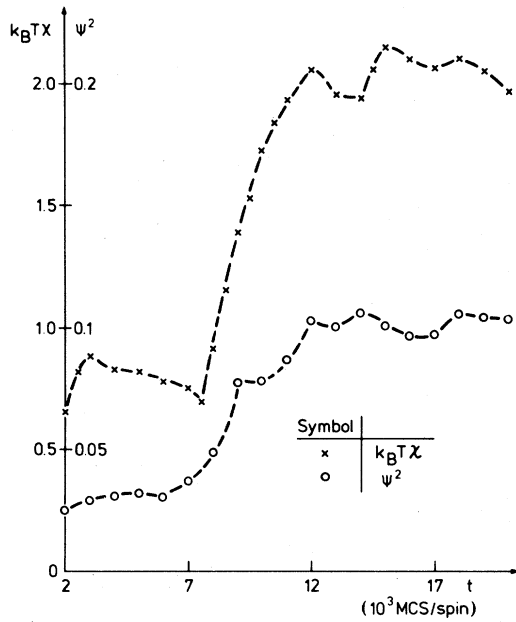


FIG. 2. Typical Monte Carlo run showing the time evolution of $k_B T \chi$ and ψ^2 for a 16×16 lattice at $k_B T/J = 1.0$. The steps during the cooling time of $t_c = 2000$ MCS/spin after the start from a random initial configuration are omitted.

shows, however, that averages where the system stays in one (or a few) of these "valleys" yield unreliable results, Fig. 3. These data based on cooling times $t_c = 2 \times 10^3$ MCS/spin and observation times $t = 2 \times 10^4$ MCS/spin are used to evaluate the Edwards-Anderson order parameter $q(t)$ (Ref. 46)

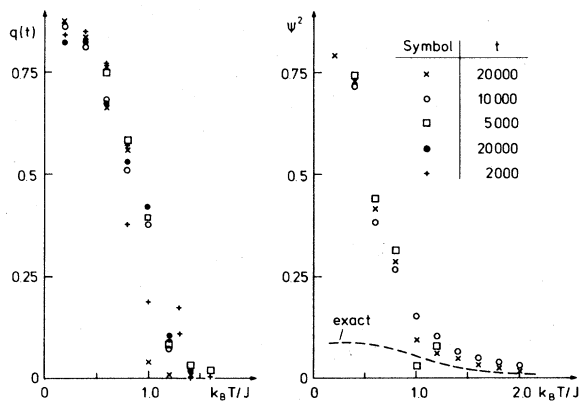


FIG. 3. Spin-glass order parameters $q(t)$ (left part) and ψ^2 (right part) plotted vs temperature, as obtained from Monte Carlo and exact calculations, for $N = 16 \times 16$. Various observation times are shown [data for $t = 2000$ MCS/spin are for $N = 80 \times 80$ (Ref. 12); these data and the full circles have random spin configurations as initial condition, while the others have a ground state as initial condition].

and time averages of $\psi_i^2(t)$. For the latter, the particular ground state $\{S_i^{(l)}\}$ was used as a starting configuration, and the results were averaged over several ground states. The results would seem to indicate that an order parameter exists at low enough temperatures, but dramatically disagree with the exact result for the chosen realization $\{J_{ij}\}$, which is also included. The exact result was obtained from the relations^{11,41}

$$\begin{aligned} \chi_{\psi}^{\mu} &= \partial^2 F / \partial (H_{\psi}^{(l)})^2, \\ \psi_i^2 &\equiv k_B T \chi_{\psi}^{\mu} / N \\ &= \sum_{i,j} S_i^{(l)} S_j^{(l)} \langle S_i S_j \rangle_T / N^2. \end{aligned} \quad (17)$$

Deliberately a realization $\{J_{ij}\}$ with fairly small ψ_i^2 was chosen to emphasize the effect that the Monte Carlo method overestimates the ordering tendency because the system stays in the vicinity of the starting ground state $\{S_i^{(l)}\}$, the corresponding "valley" in phase space, for a long time. Of course, the same effect occurs, as is well known,⁴⁷ in Monte Carlo simulations for systems with a phase transition at T_c at temperatures sufficiently below T_c ; this fact allows there the direct Monte Carlo estimation of the order parameter ψ , while in an exact calculation for a finite system there is no symmetry breaking, and hence $\langle \psi \rangle \equiv 0$ and only $\langle \psi^2 \rangle$ is meaningful (with $\lim_{N \rightarrow \infty} \langle \psi^2 \rangle = \langle \psi \rangle^2$, $\langle \psi \rangle$ being the order parameter of the infinite system, which then is well approximated by the observation ψ from a single "valley" because all valleys are equivalent). In our case where, as we will argue below, no symmetry breaking occurs at $T > 0$, the nonzero order parameter necessarily obtained from observations from single valleys is hence a spurious effect due to too small observation times, as speculatively suggested in Ref. 14. The situation is particularly deceptive, as the apparent order parameter $q(t)$ (Fig. 3, left part) seems to be fairly independent of the system size (as the $N = 80 \times 80$ data of Ref. 12 included there show), and also there is no systematic dependence on the initial state—even data with random initial state give about the same $q(t)$. In our current interpretation, this means that the system after some time just gets "locked in" in some valley of the phase space and all valleys are sufficiently narrow to produce about the same $q(t)$.

Not all quantities are seriously affected by such observation time effects. The specific heat, Fig. 4, is neither sensitive to the initial condition nor the size of the system, and for observation times considered here it agrees well with the exact result. This is to be expected, as the specific heat is mostly sensitive to short-range correlations, which come in some sort of "local equilibrium" fairly quickly.

As noted above, the exact calculation of finite systems yields $\langle \psi \rangle \equiv 0$ but on the other hand $\langle \psi^2 \rangle$ is

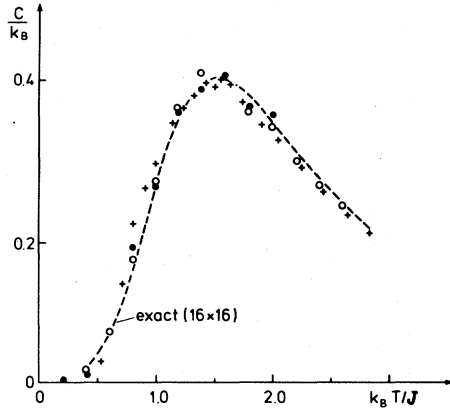


FIG. 4. Specific-heat per spin plotted vs temperature for a particular realization $\{J_{ij}\}$ of the $\pm J$ spin-glass and $N = 16 \times 16$. Monte Carlo results for runs starting either with a random spin configuration (full circles) or with a ground-state configuration (open circles). Crosses denote Monte Carlo results for $N = 80 \times 80$ of Ref. 12.

nonzero for all temperatures [from Eq. (16)]

$$\langle \psi^2 \rangle = \frac{1}{N_G} \sum_{l=1}^{N_G} \psi_l^2 = \sum_{i,j} \langle S_i S_j \rangle_0 \langle S_i S_j \rangle_T / N^2 \quad (18)$$

$$\equiv k_B T \chi_\psi / N ,$$

where N_G is the number of ground states of the system. From Eq. (18) we conclude that even for an ideal paramagnet, in the absence of any correlations, the self-terms yield $\chi_\psi = 1/k_B T$ and hence $\langle \psi^2 \rangle = 1/N$. In the presence of correlations of finite range, χ_ψ may be strongly enhanced such that $\langle \psi^2 \rangle$ is of order unity for a small system. In the case where an order parameter exists we have

$$\lim_{N \rightarrow \infty} (k_B T \chi_\psi) = N \langle \psi \rangle^2 , \quad (19a)$$

while in the case of phase transition at T_c without order parameter but infinite correlation length below T_c we expect that the sums in Eq. (18) will diverge for $N \rightarrow \infty$ to yield

$$\lim_{N \rightarrow \infty} (k_B T \chi_\psi) \propto N^x, \quad 0 < x < 1 . \quad (19b)$$

Hence it is the size dependence of $\langle \psi^2 \rangle$ which matters, and which potentially can answer the question whether an order parameter exists.

This consideration is illustrated in Fig. 5, where for comparison we include results for the Mattis³⁸ spin-glass

$$\mathcal{H}_M = -J \sum_{\langle i,j \rangle} \epsilon_i \epsilon_j S_i S_j, \quad \epsilon_i = \pm 1 , \quad (20)$$

the ϵ_i being random variables with $\langle \epsilon_i \rangle_{av} = 0$. As is well known, the disorder contained in Eq. (20) can

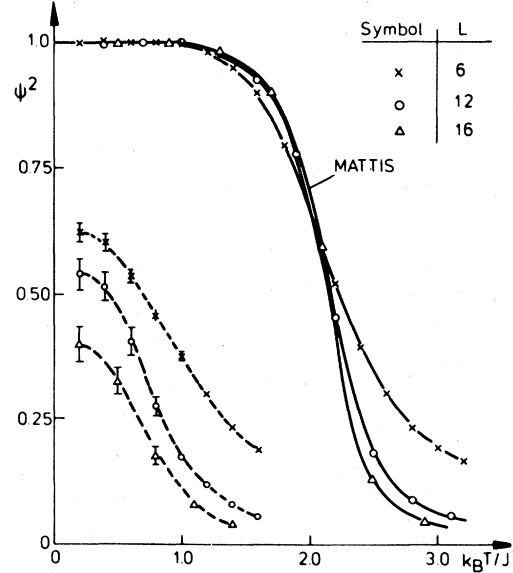


FIG. 5. Average spin-glass order parameter $(\langle \psi^2 \rangle)_{av}$ plotted vs temperature for a Mattis spin-glass (full curves) and several Edwards-Anderson spin-glass (broken curves) for several linear dimensions L . Error bars are calculated from averages over 100 realizations $\{J_{ij}\}$ for $L = 6$, 40 realizations for $L = 12$, and 25 realizations for $L = 16$.

be "gauged away" by transforming to pseudospins $S'_i = \epsilon_i S_i$, and χ_ψ in Eq. (18) thus just becomes the ferromagnetic susceptibility of the equivalent Ising ferromagnet, and $\langle \psi \rangle$ its magnetization. Figure 5 vividly illustrates that in this case the finite lattice results unambiguously show that there is an order parameter $\langle \psi^2 \rangle$ independent of lattice size at low temperatures. While above the transition (which occurs at⁴⁸ $k_B T_c/J \cong 2.27$) there is a fairly strong dependence on size due to the large short-range order contributing in Eq. (18), below T_c the effects of short-range order are much less dramatic as the long-range order saturates. Clearly, if a transition occurs at T_c where the correlation length diverges there are strong finite-size effects in the vicinity of T_c which are well understood.⁴⁹ Below T_c the correlation length decreases again and hence the finite-size effects have to become smaller as the temperature is lowered. This behavior is clearly borne out by our results for the Mattis spin-glass.

The situation for the Edwards-Anderson $\pm J$ spin-glass is very different. It is seen that $(\langle \psi^2 \rangle_T)_{av}$ always remains fairly small, and shows a pronounced size dependence at all temperatures: $(\langle \psi^2 \rangle_T)_{av}$ steadily decreases as N is increased. The saturation value $(\langle \psi^2 \rangle_0)_{av}$ decreases so strongly that we suggest

$$\lim_{N \rightarrow \infty} (\langle \psi^2 \rangle_0)_{av} = 0 ; \quad (21)$$

i.e., no order even in the ground state. Note that

this result also implies that the Edwards-Anderson order parameter

$$q = \left\langle \frac{1}{N} \sum_i \langle S_i \rangle^2 \right\rangle_{\text{av}} \quad (22)$$

is zero for $T=0$: Suppose q would be nonzero; this is only possible if a finite fraction of individual sites i has $\langle S_i \rangle^2 > 0$ in each realization $\{J_{ij}\}$. Then there is a finite fraction of the N^2 pairs $(\langle S_i \rangle \langle S_j \rangle)^2$ which is nonzero either. Hence we have the following identity, in the limit $N \rightarrow \infty$,

$$\begin{aligned} q^2 &= \left\langle \frac{1}{N} \sum_i \langle S_i \rangle^2 \right\rangle_{\text{av}} \left\langle \frac{1}{N} \sum_j \langle S_j \rangle^2 \right\rangle_{\text{av}} \\ &= \left\langle \left[\frac{1}{N} \sum_j \langle S_j \rangle^2 \right]^2 \right\rangle = \left\langle \frac{1}{N^2} \sum_{i,j} \langle S_i S_j \rangle^2 \right\rangle_{\text{av}}, \quad (23) \end{aligned}$$

since $\lim_{R \rightarrow \infty} \langle S_i S_j \rangle^2 = \langle S_i \rangle^2 \langle S_j \rangle^2$, where \bar{R} is the distance between sites ij ; in the thermodynamic limit individual realizations $\{J_{ij}\}$ lead to $q_{\{J_{ij}\}} = (1/N) \times \sum_i \langle S_i \rangle^2$ which differs from q by a negligible amount only, and hence $q^2 = (q_{\{J_{ij}\}}^2)_{\text{av}}$ holds. Now we immediately realize that Eq. (18) reduces to the right-hand side of Eq. (23) for $T=0$, and hence then the order parameters q, ψ become identical.

While the data quite clearly rule out the case Eq. (19a) it is much harder to decide whether χ_ψ in Eq. (18) is finite, and hence $(\langle \psi^2 \rangle)_{\text{av}} \propto 1/N$, or whether Eq. (19b) holds. If the correlation length ξ_ψ is finite, one expects that χ_ψ becomes independent of $N = L \times L$ if L exceeds ξ_ψ distinctly. This question is more clearly analyzed if we plot χ_ψ rather than $(\langle \psi^2 \rangle)_{\text{av}}$, Fig. 6. It is seen that data for $L=6, 12, 16$ still are nearly identical for $k_B T/J = 1.3$, the apparent freezing temperature of the Monte Carlo simulation. For $k_B T/J = 0.7$ data for $L=12, 16$ still are nearly identical, while χ_ψ for $L=6$ is distinctly smaller. Tentatively one can conclude that ξ_ψ is less than six lattice spacings at $k_B T/J = 1.3$ and less than 12 at $k_B T/J = 0.7$. Thus one has a smooth increase of correlation length, which (probably) diverges at $T=0$. Evidence that χ_ψ actually is infinite at $T=0$ has also been inferred from systematic series expansions.⁴¹

While $\chi_\psi = \chi_{EA}$ at $T=0$, this relation is no longer true at nonzero temperature. It is conceivable that $\langle S_i S_j \rangle^2$ is long ranged although $\langle S_i S_j \rangle_T$ is not.⁵⁰ In the case where an order parameter exists this would mean that the "state vector" in phase space which corresponds to an ordered phase "changes direction" when the temperature is raised. Such a behavior is known to occur in helical magnets.⁵¹ Some evidence for such a behavior was also seen in the mean-field limit of spin-glasses.⁴ Therefore it is most important to study the correlation $\langle S_i S_j \rangle^2$ directly, by help of Eq. (8).

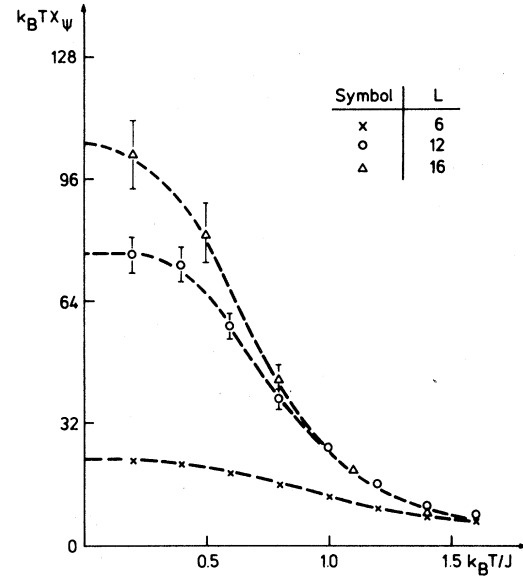


FIG. 6. Ordering susceptibility of the symmetric $\pm J$ spin-glass plotted vs temperature for various L .

This correlation is shown in log-log form in Fig. 7(a). At the lowest temperature (at about 15% of the apparent T_f seen in Monte Carlo simulations, cf. Fig. 3) the data yield a straight line, indicating a power-law decay

$$(\langle S_i S_j \rangle^2)_{\text{av}} \propto R^{-p}, \quad R \rightarrow \infty, \quad (24)$$

with $p = 0.4 \pm 0.1$. At $k_B T/J = 0.5$ (about 38% of the apparent T_f) the correlation behaves very similar for small distances, but at larger distances one sees a distinct crossover to a quicker decay. Replotting the data in semilog form [Fig. 7(b)] it is clearly seen that the data for $k_B T/J = 0.5, 0.8$ are consistent with an exponential decay

$$(\langle S_i S_j \rangle^2)_{\text{av}} \propto \exp(-R/\xi_{EA}), \quad R \rightarrow \infty. \quad (25)$$

The different behavior of $k_B T/J = 0.2$ at this plot could indicate that a phase transition from exponential decay to power-law decay occurs at some temperature $k_B T_c/J$ between 0.2 and 0.5, as in the two-dimensional XY model.⁵² We consider this possibility unlikely, for the following reasons: Our data for χ_ψ have already indicated that ξ_ψ becomes of order 10 lattice spacings at $k_B T/J \approx 0.7$, and is steadily increasing with decreasing temperature. Due to Eq. (24) we expect that $\xi_{EA} \geq \frac{1}{2} \xi_\psi$, and hence at $k_B T/J = 0.2$ we clearly have $\xi_{EA} \gg L$. Hence for the distances $|\bar{r}_{ij}|$ available we do not expect to see any effect of the exponential decay, Eq. (25), and the crossover from Eq. (24) to Eq. (25) occurs in Fig. 7(a) for much larger distances than are available from this type of numerical calculation. If there were

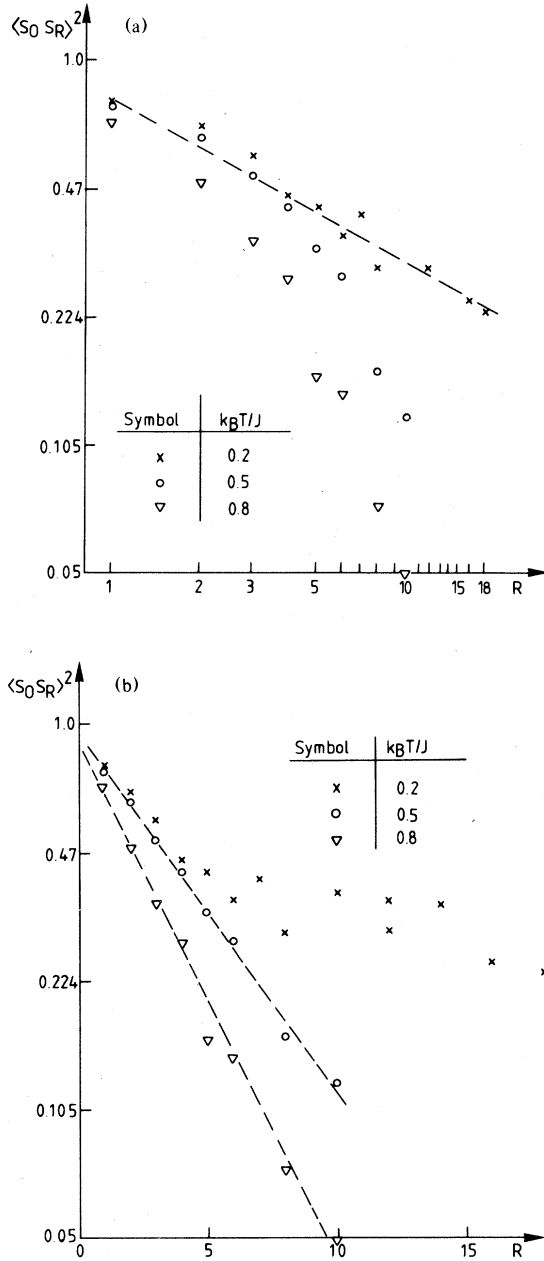


FIG. 7. Correlation function $\langle S_0 S_R \rangle^2 \equiv [\langle S_i S_j \rangle_T^2]_{av}$ plotted vs R in log-log form (a) and semilog form (b) for three temperatures.

a phase transition from Eq. (24) to Eq. (25) at a $T_c > 0$, the possible T_c would be about $\frac{1}{10}$ (or less) of the transition temperature of the corresponding Mattis spin-glass.

Finally, we note the relation between the exponents x, p defined in Eqs. (19b) and (24). Since χ_ψ for $N \rightarrow \infty$ diverges, one can replace the summations by integrals over the volume V of the system

(measuring lengths in units of the lattice spacing)

$$\begin{aligned} \langle (\psi^2)_0 \rangle_{av} &= \frac{1}{N} \int_V d\vec{r}_{ij} \langle (S_i S_j)_0^2 \rangle_{av} \\ &\propto \frac{1}{N} \int_0^{\sqrt{N}} r^{1-p} dr \propto N^{-p/2}, \end{aligned} \quad (26)$$

and hence $x = p/2$.

The behavior found here is of the same type as in the (fully frustrated) Ising antiferromagnet on the triangular lattice, where⁵³ $p = 1$.

IV. NUMERICAL RESULTS FOR THE SYMMETRIC GAUSSIAN MODEL AND A COMPARISON WITH MONTE CARLO SIMULATIONS

Again we start by comparing the internal energy obtained from the exact method with Monte Carlo results, Fig. 8(a). While the simulation data are in fair agreement with the exact calculation at high temperatures, deviations start relatively soon below the apparent freezing temperature ($k_B T_f/\Delta J \approx 1.0$ here⁹), and at low temperatures the deviations are quite pronounced. Our estimate, based on extrapolating the average ground-state energy of $L \times L$ lattices to $L \rightarrow \infty$ [Fig. 1(b)]

$$E(T=0)/J = -1.31 \pm 0.01, \quad (27)$$

is significantly lower than previous values $E(T=0)/J = -1.25$ (Refs. 15 and 19). Our methods to find the ground state in principle work here also, but in practice it was much harder to obtain the ground states: we find that their degeneracy is only twofold (i.e., reversal of the signs of all the spins), but there are many metastable states with only slightly higher energy. This result, of course, has to be expected: for a finite lattice we have a finite number ($2LK - K$ in our case) of exchange constants $\{J_{ij}\}$ drawn from a Gaussian distribution. The energy is a linear combination of these $2LK - K$ real numbers in every spin configuration, where due to the pairwise character of the interaction and $S_i = \pm 1$ the same linear combination is obtained if $S_i \rightarrow -S_i$ for all spins simultaneously. On the other hand, the probability that two different linear combinations have precisely the same energy is zero. A higher degeneracy, however, may be recovered in the thermodynamic limit where then low-lying metastable states may merge with the ground state. Figure 8(b) shows the temperature variation of the entropy. Since the ground state is twofold degenerate, we expect $S(T=0)/k_B = \ln 2/N$. The data are consistent with this behavior. Disregarding this finite-size behavior, we find that the entropy is represented by a linear variation, $S(T)/k_B \approx 0.3 k_B T/\Delta J$, over a wide range of temperatures. Since $dS/d(k_B T/\Delta J) = C \Delta J/k_B T$, this fact implies also a linear variation of the specific

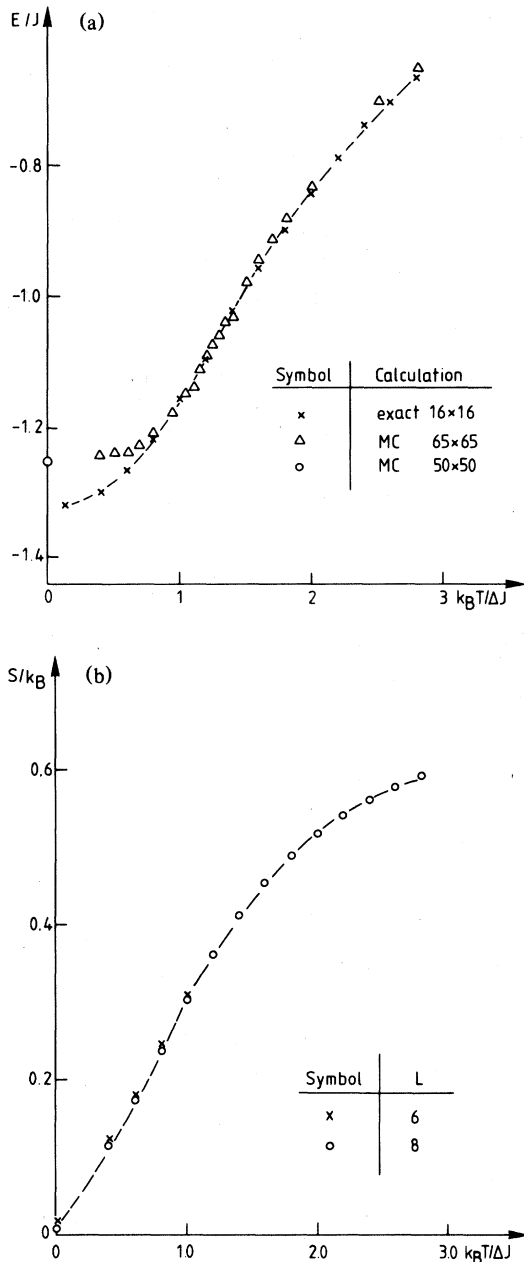


FIG. 8. (a) Internal energy of the symmetric Gaussian model plotted vs temperature for a 16×16 lattice. Monte Carlo data for the 65×65 system are from Ref. 9 and for the 50×50 system from Ref. 15. (b) Entropy plotted vs temperature for two $L \times L$ lattices.

heat at low temperatures, which agrees with its direct observations (see Fig. 11 below).

Due to this low degeneracy of the exact ground states the behavior of the order parameter is quite different from that in the $\pm J$ model, Fig. 9. Although 16 realizations of a 16×16 lattice were generated, due to the above mentioned difficulties

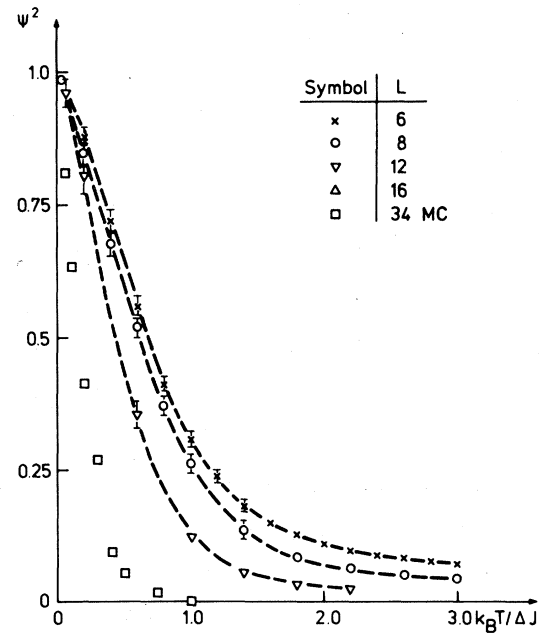


FIG. 9. Average spin-glass order parameter $(\langle \psi^2 \rangle)_{av}$ plotted vs temperature for a symmetric Gaussian spin-glass according to exact calculation for various $L \times L$ lattices and Monte Carlo (Ref. 11). Error bars are calculated from averages over 40 realizations $\{J_{ij}\}$ for $L=6, 8$, and 20 realizations for $L=12$.

only for two of them a ground state was found, and hence they are omitted here. But it is interesting to note that even the 34×34 Monte Carlo data,¹¹ where almost certainly not the projection on ground states but rather on metastable states was used to compute an "order parameter," fit well to the picture. We hence note that again there is a systematic trend with the size of the system, which was not seen in the earlier Monte Carlo data^{11,15} due to their large statistical fluctuations and observation time and effects. However, from Fig. 9 we now conclude

$$\lim_{N \rightarrow \infty} (\langle \psi^2 \rangle_{T=0}) = 1, \quad \lim_{N \rightarrow \infty} (\langle \psi^2 \rangle_{T>0}) = 0 ; \quad (28)$$

i.e., at nonzero temperatures there is no order parameter in the Gaussian model either, while there is one [in the sense implied by Eq. (28)] at zero temperature, in contrast to the $\pm J$ model.

In Fig. 10 the data for $k_B T \chi_\psi$ are given. The susceptibility increases smoothly with decreasing temperature. Near the apparent freezing temperature $k_B T/\Delta J = 1$ the data for $L=8, 12$ nearly agree while the result for $L=6$ is somewhat smaller. This indicates that $\xi_\psi \approx L=6$ close to that temperature.

Again the Monte Carlo method, although it overemphasizes the order due to restricted observation time, yields fairly reliable estimates for the specific heat, Fig. 11. As expected, finite-size effects

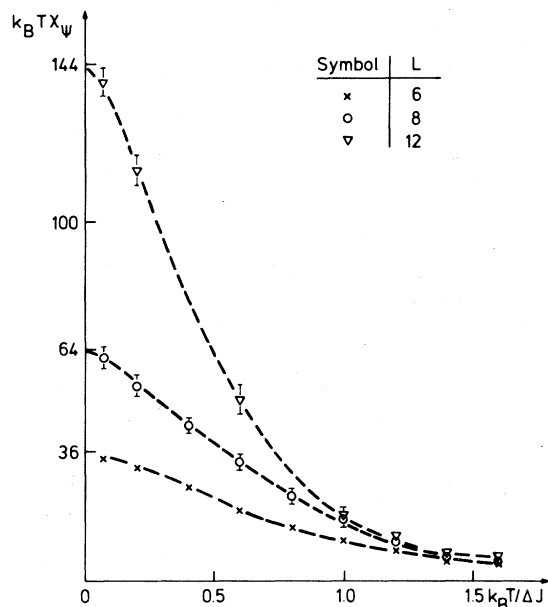


FIG. 10. Ordering susceptibility of the symmetric Gaussian spin-glass plotted vs temperature for various L .

have little effect on the specific heat, as in the case of the $\pm J$ model. We expect some systematic size dependence at very low temperatures, from the argument about the degeneracy of energy levels given above: for any finite system, the first excited energy level differs from the ground state by a small but finite relative amount c ($c \propto 1/\sqrt{N}$), and hence the specific heat must vary according to an exponential, $C/k_B \propto \exp[-cE(T=0)/k_B T]$. In the thermodynamic limit the gap may vanish and the specific heat may vary according to a power law, $C/k_B \propto T^y$. The numerical results of Fig. 11 at $k_B T \gg cE(T=0)$ suggest a linear variation ($y=1$), in surprising agreement with experiment.^{8,54} Note that in the $\pm J$ model excitations only in integer steps of J are possible and a strong exponential variation of C remains in the thermodynamic limit (cf. Fig. 11).

The correlation function is nicely consistent with a smooth exponential decay at all temperatures considered, Fig. 12, and from the above considerations [Eqs. (22) and (23)] we conclude that the Edwards-Anderson order parameter is zero for $T \neq 0$ while it is nonzero at $T=0$. Again it is not possible to clearly distinguish whether Eq. (24) or Eq. (25) holds at very low temperatures, but for temperatures exceeding 20% of the apparent freezing temperature of the Monte Carlo simulations the exponential decay, Eq. (25), is already clearly favored. From Fig. 12(b), we expect that at our lowest temperatures ξ_{EA} distinctly exceeds the largest L 's and distances R available, and hence much larger systems would be required to check the exponential decay unambiguously. Our

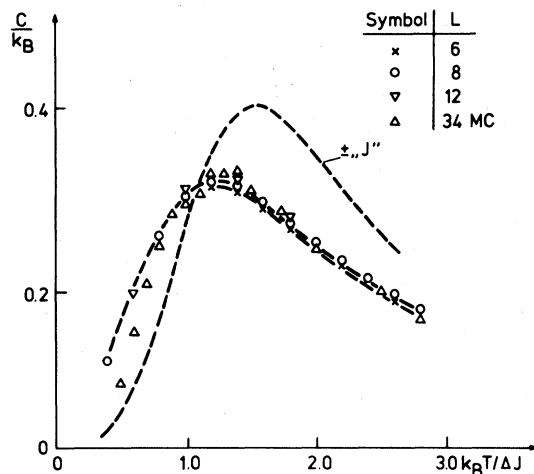


FIG. 11. Specific heat of the symmetric Gaussian spin-glass plotted vs temperature as obtained from the exact calculation of various $L \times L$ lattices. Monte Carlo data for $L=34$ from Ref. 11 are included for comparison, as well as the specific-heat curve of the $\pm J$ model.

findings corroborate recent studies by Reed,⁵⁵ where Onsager's⁴⁸ exact solution of the Ising model with homogeneous exchange was generalized to lattices where a $L \times L$ cell (with arbitrary couplings inside the cell) is periodically repeated: for $L \leq 5$ he finds that the temperature of the specific-heat singularity decreases strongly with increasing L , and his numerical data would be hard to reconcile with a transition for $L \rightarrow \infty$ at $k_B T/J = 1.0$, although he cannot rule out a transition at much smaller temperatures. We hence conclude that the apparent transition in Monte Carlo simulations of two-dimensional Ising spin-glasses is an observation time effect, but emphasize the point^{15,16} that the Monte Carlo evidence on this question in itself is very ambiguous, and one must be careful in drawing conclusions on other dimensionalities.

Figure 13, finally, presents the temperature dependence of the correlation length as estimated from results as shown in Figs. 7 and 12. It is seen that the data are consistent with a divergence of the correlation length for $T \rightarrow 0$.

Defining a correlation length ξ_{EA} from the second moment of the correlation function

$$\xi_{EA}^2 = \sum_{i,j} R^2 (\langle S_i S_j \rangle)_{av} / (N k_B T \chi_{EA}) \quad (29)$$

one immediately obtains for a lattice of coordination number z in leading order of high-temperature expansion

$$\xi_{EA} \approx \sqrt{z} \frac{1}{k_B T} [(J^2)_{av}]^{1/2} \quad (30)$$

Hence for the symmetric $\pm J$ model the asymptotic

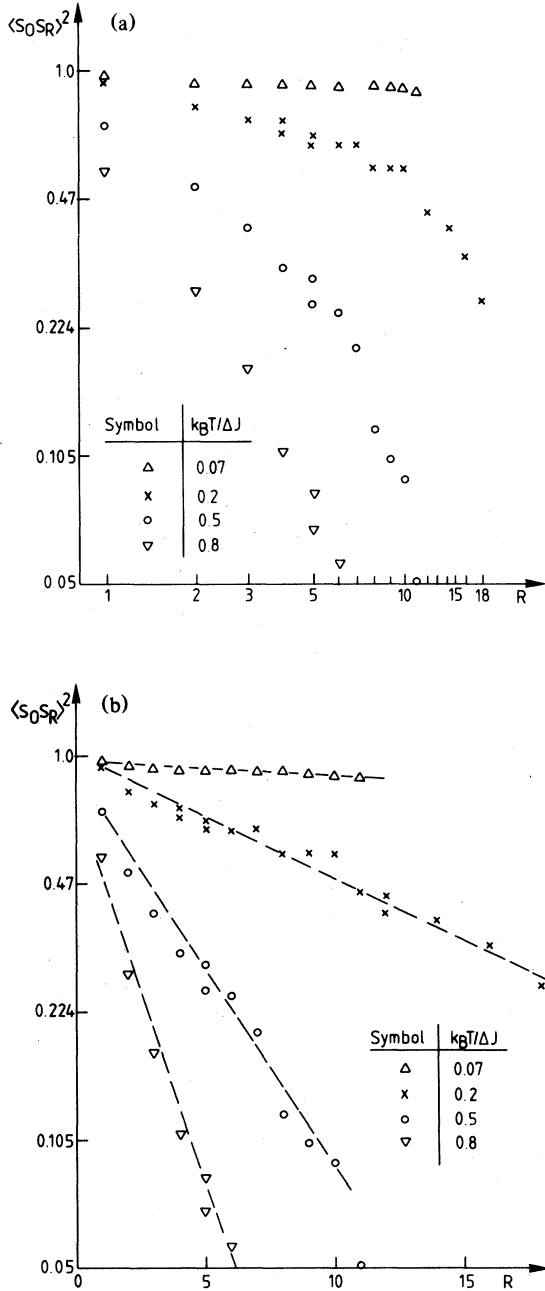


FIG. 12. Correlation function $\langle S_0 S_R \rangle^2 \equiv (\langle S_i S_j \rangle_T^2)_{av}$ plotted vs R in log-log form (a) and semilog form (b) for several temperatures.

behavior of the correlation length is simply $\xi_{EA} = 2J/k_B T$ while for the Gaussian model $\xi_{EA} = 2\Delta J/k_B T$. These forms are included in Fig. 13 to demonstrate that for large $k_B T/J$ (or $k_B T/\Delta J$) the correct asymptotic behavior is approached. We did not attempt to carry the high-temperature analysis to higher order as already the series for χ_{EA} is quite irregular.^{28,29}

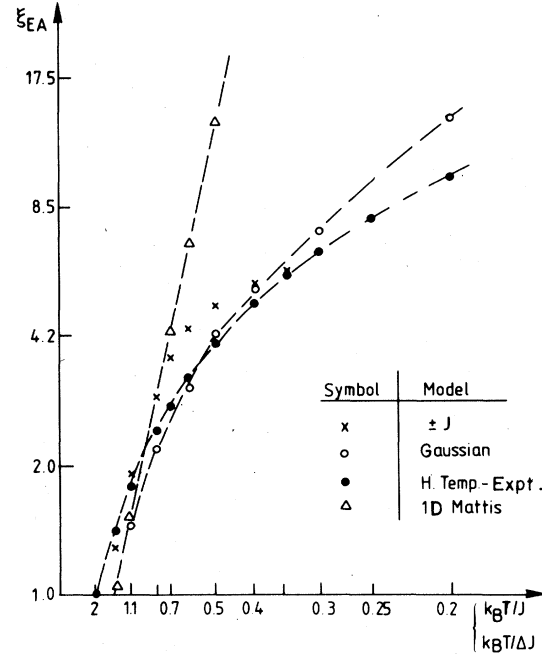


FIG. 13. Correlation length ξ_{EA} plotted vs reciprocal temperature for both the Gaussian and the $\pm J$ spin-glass. Curve with black dots indicates the asymptotic behavior for $1/T \rightarrow 0$.

V. ASYMMETRIC $\pm J$ MODEL AND THE TRANSITION TO THE FERROMAGNETIC PHASE

In the asymmetric $\pm J$ model it makes sense to study the ferromagnetic susceptibility

$$k_B T \chi_F = k_B T (\partial^2 F / \partial H^2) = \sum_{i,j} (\langle S_i S_j \rangle)_{av} / N$$

(while in the symmetric case we trivially have $\chi_F = 1/k_B T$). Figure 14 shows our numerical results for several concentrations x of negative bonds. Arguing similarly as for χ_ψ above, we conclude that $k_B T \chi_F / N$ is related to the square of the magnetization M . It is seen that $k_B T \chi_F$ decreases monotonically with temperature, as well as with concentration x . Within our accuracy there is no evidence of a double transition paramagnet \rightarrow ferromagnet \rightarrow spin-glass (or paramagnet?), seen in some experimental systems.⁸ In order to estimate from the data in Fig. 14 where precisely the transition paramagnet-ferromagnet occurs, a careful analysis of the size dependence is necessary, of course. Figure 15 shows the concentration dependence of the magnetization at $k_B T/J = 0.2$ (which agrees with the ground-state magnetization to within our accuracy, cf. Fig. 14). We estimate the transition ferromagnet-paramagnet for

$$x_f \approx 0.33 \pm 0.03 \quad (x_c \approx 0.12 \pm 0.015), \quad (31)$$

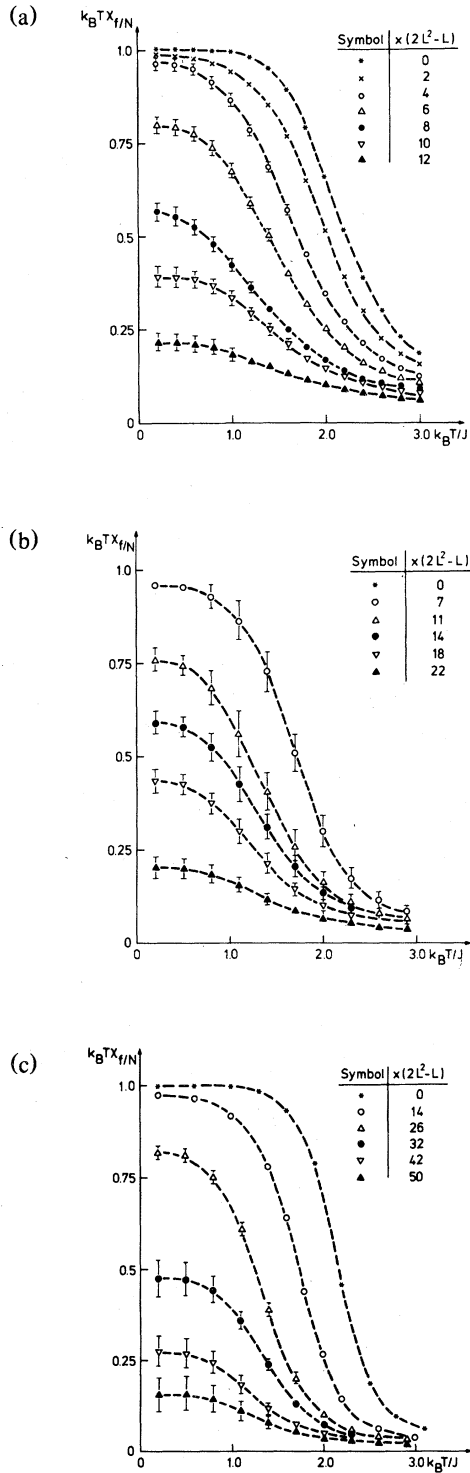


FIG. 14. Average magnetization $(M^2)_{av}$ plotted vs temperature for various concentrations x of negative bonds and three lattice sizes $N = L \times L$: $L = 6$, 50 realizations (a); $L = 8$, 40 realizations (b); $L = 12$, 25 realizations (c). Note that for our boundary conditions the total number of bonds is $2L^2-L$.

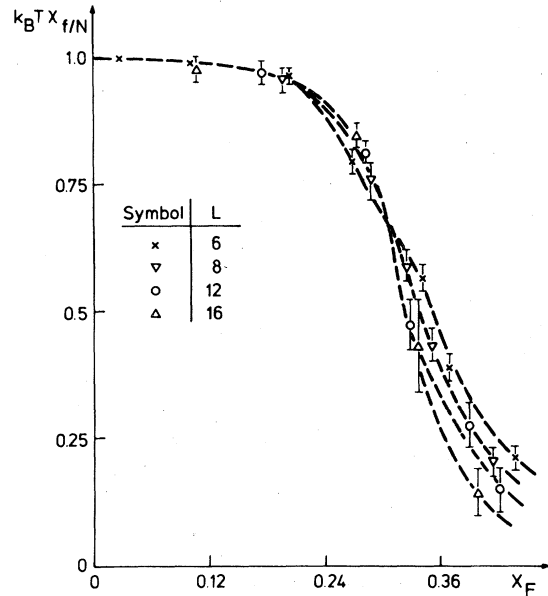


FIG. 15. Average magnetization $(M^2)_{av}$ plotted vs concentration x_F of frustrated plaquettes at $k_B T / J = 0.2$ for various $L \times L$ lattices. Arrow marks estimated transition of the infinite system.

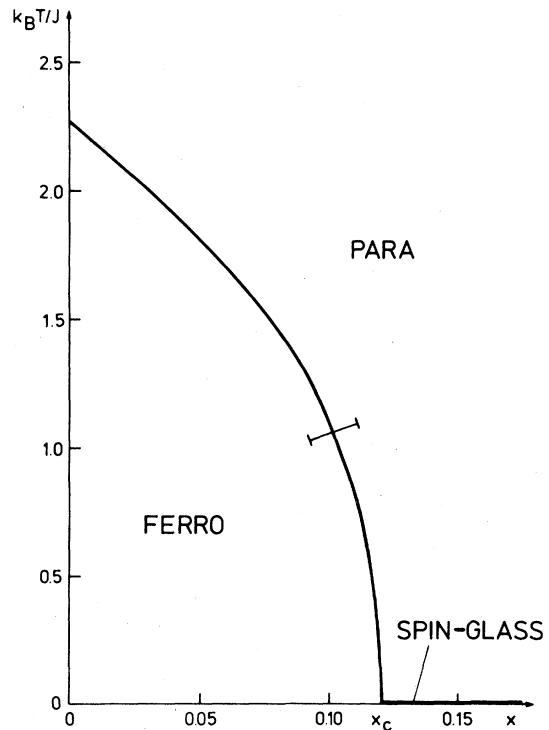


FIG. 16. Phase diagram of the $\pm J$ model. Error bar represents the typical uncertainty in the location of the phase boundary.

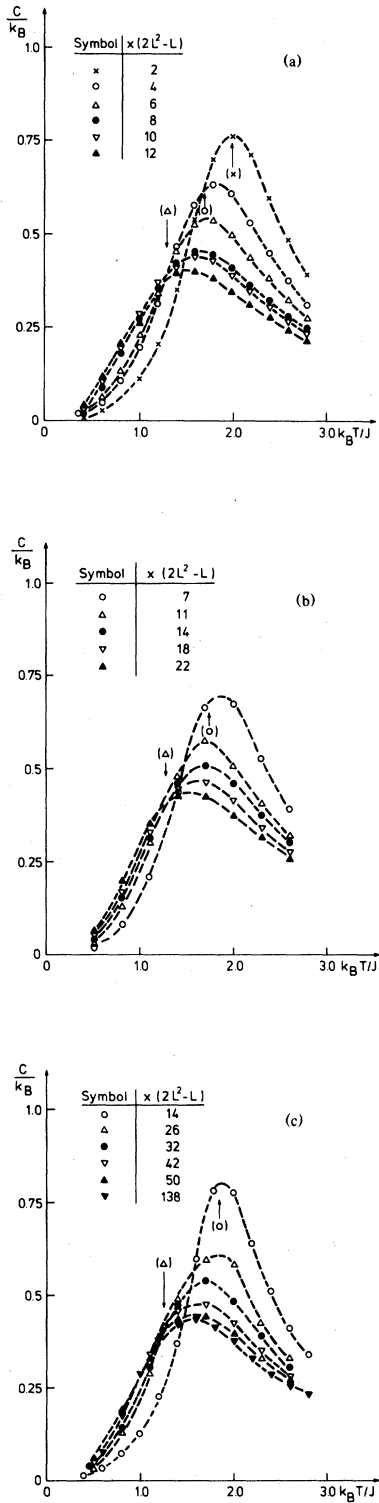


FIG. 17. Average specific heat plotted vs temperature for various concentrations x of negative bonds and three lattice sizes: $L = 6$, 50 realizations (a); $L = 8$, 40 realizations (b); $L = 12$, 25 realizations (c). Arrows mark the position of the phase boundary drawn in Fig. 16.

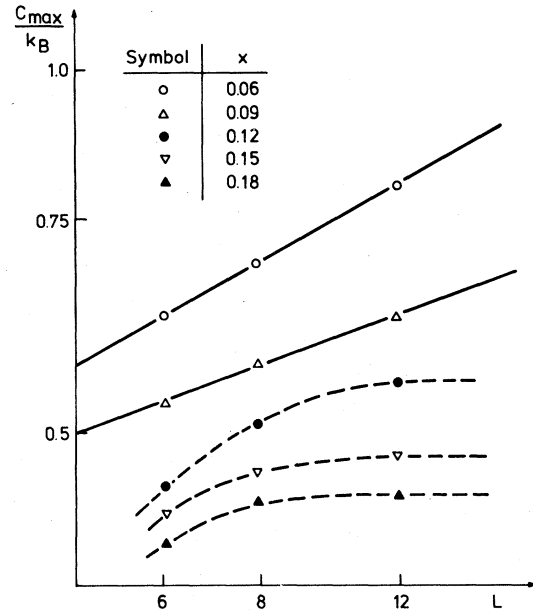


FIG. 18. Log-log plot of the specific-heat maximum vs linear dimension of the system for various concentrations x . Curves are only drawn to guide the eye.

which is in the range of previous estimates [$x_c \approx 0.1$ (Ref. 32), $x_c = 0.145 \pm 0.005$ (Ref. 33), $x_c \approx 0.15$ (Ref. 45), $x_c \approx 0.15-0.20$ (Ref. 12)]. The resulting phase diagram (Fig. 16) is hence qualitatively similar to that obtained by Young⁵⁶ from real-space renormalization.

Figure 17 finally analyzes the behavior of the specific heat. It is seen that the position of the specific-heat maximum coincides with the phase boundary for small x only. Presumably the specific-heat divergence is dominating the behavior in the thermodynamic limit in a very narrow temperature interval around the transition only, as it happens in noncompeting dilute ferromagnets.⁵⁷ In a finite system, such a singularity is completely wiped out by rounding effects, but a broad background Schottky anomaly remains (its maximum is not related to any transition, cf. Fig. 14). This interpretation is corroborated by the fact that for larger x the specific heat very quickly approaches that of the symmetric $\pm J$ model [which is also included in Fig. 17(c)]. Figure 18 shows that the specific-heat maxima increase with L for small x steadily, while for larger x they first increase but then saturate: favoring again the interpretation that in this case, the specific-heat peak is due to (ferromagnetic) clusters occurring above the transition (if a transition occurs at all).

VI. CONCLUSIONS

We briefly summarize the main findings of this work as follows:

(i) Both the two dimensional $\pm J$ and the Gaussian spin-glass model have a thermodynamic phase transition at zero temperature only, at nonzero temperatures all spin-glass order parameters are zero. In the $\pm J$ model the order parameters are zero even at zero temperature, but there the correlation function $(\langle S_i S_j \rangle)^2_{av}$ decays with an inverse-power law of distance, while in the Gaussian model at $T=0$ the order parameters are unity. At nonzero temperature this correlation function decays exponentially with distance, and the associated correlation length diverges for $T \rightarrow 0$. The limiting high-temperature approximation $\xi_{EA} \approx 2(J/k_B T)$ [or $2(\Delta J/k_B T)$ in the Gaussian case, respectively] gives a surprisingly good representation over a broad range of temperatures. The divergence of the correlation length is hence much weaker than in the (frustrationless) one-dimensional case. Note that there the correlation length diverges exponentially fast, as expected for a system at its lower critical dimensionality (lcd). Our results suggest that the correlation length of the *frustrated* spin-glass models diverges for $T \rightarrow 0$ as a power law of temperature only, just as the one-dimensional n -vector models for $n \geq 2$. Since there the dimensionality is lower than the lower critical one (lcd = 2 there), our findings do not contradict the suggestion that $d=2$ is below, not at, the lower critical dimensionality of a frustrated Ising spin-glass.

(ii) The entropy of the $\pm J$ spin-glass reaches a positive nonzero value at $T=0$ ($S/k_B \approx 0.075$), in good agreement with estimates obtained by other approaches. In the Gaussian case we find $S(T=0) = 0$ (in the thermodynamic limit), and both S and the specific heat vary *linearly* over a wide range of temperature. This fact was not so clear from earlier Monte Carlo studies of this model, which were hampered by slow relaxation effects at low temperatures, while at higher temperatures our results agree well with the Monte Carlo estimates. For the $\pm J$ model the specific heat agrees nicely with Monte Carlo data at all temperatures but there the specific heat varies exponentially at low temperatures. Note that our results for the entropy comply with the "rule" that a nonzero ground-state entropy indicates absence of ground-state order, while zero entropy implies order.

(iii) The phase boundary ferromagnet-paramagnet of the $\pm J$ model is estimated as function of the concentration x of negative bonds (Fig. 16). We find that

ferromagnetism vanishes at $x_c \approx 0.12$, in fair agreement with other approaches.

(iv) The time scales necessary to reach equilibrium in a Monte Carlo simulation have been identified, and they are found to increase dramatically with increasing system size at low temperatures. Since there are good reasons that the Monte Carlo dynamics of a spin-glass simulates the actual dynamics reasonably well (cf. Ref. 11), we expect that also macroscopic real spin-glass samples will be characterized by an incomplete thermal equilibrium of the spins. The system stays for a fairly long time in the vicinity of one of its ground states (or low-lying metastable states) until it experiences a transition into another preferred "valley" in configuration space by a rearrangement of large clusters of spins. The behavior differs from the Néel picture of "magnetic clouds,"⁵⁸ however, because the "clusters" are not isolated well-identifiable objects, but rather interacting, overlapping, etc., spins belonging to one cluster at a time, may belong to another one at a later time, etc. The gradual increase of magnetic correlations as temperature is lowered is much more precisely characterized by the correlation length studied for the present models. The peak in the frequency dependent susceptibility for the present models do set in at fairly well-defined "freezing temperatures", as the mentioned Monte Carlo simulations have shown: below these temperatures, Edwards-Anderson-type order is *metastable* for fairly long times (Figs. 2 and 3).

In conclusion then, we feel that the behavior of two-dimensional Ising spin-glasses is fairly well understood—although it would be nice, of course, to make our calculations more accurate and go to larger systems. However, since the present study needed about 500 h computing time at an IBM 370/168 machine, a straightforward extension of our techniques is not easy.

ACKNOWLEDGMENTS

We have benefited from fruitful discussions and/or correspondence with J. Vannimenus, D. Stauffer, A. Aharony, D. J. Thouless, S. Kirkpatrick, B. I. Halperin, and M. A. Moore. We thank the latter as well as S.-K. Ma, R. Maynard, G. Parisi, L. P. Kadanoff, J. Villain, and P. Reed for sending unpublished reports of their work.

¹For recent reviews see: P. W. Anderson, *J. Appl. Phys.* **49**, 1599 (1978), and in *Amorphous Magnetism II*, edited by R. A. Lewy and R. Hasegawa (Plenum, New York, 1977), p. 1; A. Blandin, *J. Phys. (Paris)* **39**, C6-1499 (1978); K. Binder, *ibid.* **39**, C6-1527 (1978), and in *Ordering in Strongly Fluctuating Condensed-Matter Systems*, edited by T. Riste (Plenum, New York, 1979); C. de Dominicis,

Dynamic Critical Phenomena (Springer, Berlin, 1979).

²S. F. Edwards and P. W. Anderson, *J. Phys. F* **5**, 965 (1975).

³D. Sherrington and S. Kirkpatrick, *Phys. Rev. Lett.* **35**, 1792 (1975).

⁴D. J. Thouless, P. W. Anderson, and R. G. Palmer, *Philos. Mag.* **35**, 593 (1977).

- ⁵H.-J. Sommers, Z. Phys. B 31, 301 (1978); B 32, 173 (1979).
- ⁶A. J. Bray and M. A. Moore, Phys. Rev. Lett. 41, 1068 (1978), and (unpublished); see also C. de Dominicis and T. Garel, J. Phys. Lett. 24, L575 (1979).
- ⁷G. Parisi, Phys. Rev. Lett. 43, 1754 (1979), and (unpublished).
- ⁸For recent review of experimental work on spin-glasses, see, e.g., J. A. Mydosh, J. Magn. Magn. Mater. 7, 237 (1978), and in *Amorphous Magnetism II*, edited by R. A. Lewy and R. Hasegawa (Plenum, New York, 1977), p. 73; P. A. Beck, Prog. Mater. Sci. 23, 1 (1978); A. P. Murani, J. Phys. (Paris) 39, C6-1517 (1978), and J. Appl. Phys. 49, 1604 (1978); J. Souletie, J. Phys. (Paris) 39, C2-3 (1978).
- ⁹K. Binder and K. Schröder, Phys. Rev. B 14, 2142 (1976).
- ¹⁰K. Binder and D. Stauffer, Phys. Lett. A 57, 177 (1976).
- ¹¹K. Binder, Z. Phys. B 26, 339 (1977).
- ¹²S. Kirkpatrick, Phys. Rev. B 16, 4630 (1977).
- ¹³S. Kirkpatrick, in *Ordering in Strongly Fluctuating Condensed-Matter Systems*, edited by T. Riste (Plenum, New York, 1979).
- ¹⁴A. J. Bray and M. A. Moore, J. Phys. F 7, L333 (1977); A. J. Bray, M. A. Moore, and P. Reed, J. Phys. C 11, 1187 (1978).
- ¹⁵D. Stauffer and K. Binder, Z. Phys. B 30, 313 (1978).
- ¹⁶D. Stauffer and K. Binder, Z. Phys. B 34, 97 (1979).
- ¹⁷J. S. Denbigh (unpublished).
- ¹⁸A. J. Bray, M. A. Moore, and P. Reed, J. Phys. C 12, L447 (1979).
- ¹⁹C. Dasgupta, S.-K. Ma, and C.-K. Hu, Phys. Rev. B 20, 3837 (1979).
- ²⁰R. Rammal, R. Suchail, and R. Maynard, Solid State Commun. 32, 487 (1979).
- ²¹J. F. Fernandez and R. Medina, Phys. Rev. B 19, 3561 (1979).
- ²²P. W. Anderson and C. M. Pond, Phys. Rev. Lett. 40, 903 (1978).
- ²³W. Kinzel and K. H. Fischer, J. Phys. C 11, 2115 (1978), and references therein.
- ²⁴A. B. Harris, T. C. Lubensky, and J. H. Chen, Phys. Rev. Lett. 36, 415 (1976).
- ²⁵E. Pytte and J. S. Rudnick, Phys. Rev. B 19, 3603 (1979).
- ²⁶J. R. de Almeida and D. J. Thouless, J. Phys. A 11, 983 (1978).
- ²⁷A. J. Bray and M. A. Moore, J. Phys. C 12, 79 (1979).
- ²⁸R. Fisch and A. B. Harris, Phys. Rev. Lett. 38, 785 (1977).
- ²⁹R. V. Ditzian and L. P. Kadanoff, Bull. Am. Phys. Soc. 24, (1979), and (private communication).
- ³⁰G. Toulouse, Commun. Phys. 2, 115 (1977).
- ³¹J. Vannimenus and G. Toulouse, J. Phys. C 10, L537 (1977).
- ³²J. Vannimenus and L. de Séze (unpublished).
- ³³I. Bieche, R. Maynard, R. Rammal, and J. P. Uhry, J. Phys. A (in press).
- ³⁴P. Reed, A. J. Bray, and M. A. Moore, J. Phys. C 11, L139 (1978).
- ³⁵B. Derrida, J. M. Maillard, J. Vannimenus, and S. Kirkpatrick, J. Phys. (Paris) 39, L465 (1978).
- ³⁶I. E. Dzyaloshinskii and G. E. Volovik, J. Phys. (Paris) 39, 693 (1978).
- ³⁷J. A. Hertz, Phys. Rev. B 18, 4875 (1978).
- ³⁸D. C. Mattis, Phys. Lett. A 56, 421 (1976); J. M. Luttinger, Phys. Rev. Lett. 37, 778 (1976); A. Aharony and Y. Imry, Solid State Commun. 20, 899 (1976).
- ³⁹J. Villain, Les Houches Lecture Notes 1978 (in press).
- ⁴⁰D. J. Elderfield (unpublished).
- ⁴¹A. Aharony and K. Binder, J. Magn. Magn. Mater. (in press), and (unpublished).
- ⁴²A very brief account of some of our results was given earlier in I. Morgenstern and K. Binder, Phys. Rev. Lett. 43, 1615 (1979).
- ⁴³K. Binder, Physica (Utrecht) 62, 508 (1972).
- ⁴⁴In models with random magnetic fields one rather keeps the exchange J constant and Eq. (9) has to be replaced by $(\dots)_{av} = \prod_i \int dH_i P(H_i) \dots$; applications of our method to this case will be described elsewhere.
- ⁴⁵I. Ono, J. Phys. Soc. Jpn. 41, 345 (1976); see also, E. Domany, J. Phys. C 12, L119 (1979), who obtains $x_c \approx 0.16$ from replica methods.
- ⁴⁶The definition of the Edwards-Anderson order parameter in Monte Carlo simulations is discussed in Refs. 9–11 and 15.
- ⁴⁷*Monte Carlo Methods in Statistical Physics*, edited by K. Binder (Springer, Berlin, 1979).
- ⁴⁸L. Onsager, Phys. Rev. 65, 117 (1944).
- ⁴⁹M. E. Fisher, in *Critical Phenomena*, edited by M. S. Green (Academic, New York, 1971).
- ⁵⁰One of us (K.B.) is indebted to helpful discussions with B. I. Halperin and D. J. Thouless on this point.
- ⁵¹W. Selke and M. E. Fisher, Phys. Rev. B 20, 257 (1979); P. Bak and J. von Boehm (unpublished).
- ⁵²J. M. Kosterlitz and D. J. Thouless, J. Phys. C 6, 1181 (1973).
- ⁵³J. Stephenson, J. Math. Phys. 11, 420 (1970).
- ⁵⁴D. Meschede, F. Steglich, H. Maletta, and W. Zinn, Phys. Rev. Lett. 44, 102 (1980).
- ⁵⁵P. Reed, J. Phys. C 12, L799 (1979).
- ⁵⁶A. P. Young, in *Amorphous Magnetism II*, edited by A. R. Lewy and R. Hasegawa (Plenum, New York, 1977).
- ⁵⁷C. Jayaprakash, E. K. Riedel, and M. Wortis, Phys. Rev. B 18, 2244 (1978); H. A. Algra, L. J. de Jongh, and J. Reedijk, Phys. Rev. Lett. 42, 6061 (1979).
- ⁵⁸L. Néel, Ann. Geophys. 5, 99 (1979); J. L. Tholence and R. Tournier, J. Phys. (Paris) 35, C4-229 (1974); P. A. Beck, in Ref. 8.